Keyholes, Correlations, and Capacities of Multielement Transmit and Receive Antennas

Dmitry Chizhik, Gerard J. Foschini, *Fellow, IEEE*, Michael J. Gans, *Fellow, IEEE*, and Reinaldo A. Valenzuela, *Fellow, IEEE*

***Abstract*—Multielement system capacities are usually thought of as limited only by correlations between elements. It is shown here that degenerate channel phenomena called "keyholes" may arise under realistic assumptions which have zero correlation between the entries of the channel matrix H and yet only a single degree of freedom. Canonical physical examples of keyholes are presented. For outdoor environments, it is shown that roof edge diffraction is perceived as a "keyhole" by a vertical base array that may be avoided by employing instead a horizontal base array.**

***Index Terms*—Bell-labs layered space–time, correlation, keyhole, multiple-input multiple-output, propagation.**

I. Introduction

SINGLE USER communication with M transmit and N receive antennas can achieve very high spectral efficiencies in highly scattering environments [1]. For example, Bell-labs layered space–time (BLAST) communication technique has been proposed by Foschini [2], and demonstrated experimentally by Golden *et al.* [3] and Wolniansky *et al.* [4]. These high spectral efficiencies are enabled by the fact that a scattering environment makes the signal from every individual transmitter appear highly uncorrelated at each of the receive antennas. As a result, the signal corresponding to every transmitter has a distinct spatial signature at the receiver. These different spatial signatures allow the receiver to effectively separate, with adequate signal processing, the transmissions—simultaneously and on the same frequency—by the different transmit antennas. In a sense, the scattering environment acts like a very large aperture that makes it possible for the receiver to resolve the individual transmitters.

The high spectral efficiency is reduced if the signals arriving at the receivers are correlated. A narrow-band channel may be described in terms of a complex channel transfer matrix $\mathbf{H}$, whose entry h_{nm} corresponds to the response of the nth receiver to the signal sent by the mth transmitter. When the entries of $\mathbf{H}$ are distributed as complex Gaussians, maximum capacity is achieved when $\langle h_{nm}h_{kl}^{*}\rangle = 0$ for $n \neq k$ and $m \neq l$. Correlation between antennas may be reduced in actual deployments by separating the antennas spatially [5]–[7]. However, it has been shown by Chizhik *et al.* [8] and by Gesbert *et al.* [9] that low correlation is not a guarantee of high capacity. In [8], the existence of degenerate channels called "keyholes" has been proposed and demonstrated through physical examples that have uncorrelated transmit and receive signals, and yet only a single degree of freedom. In [9], it has been shown that such degenerate channels termed "pinholes", are extreme cases in a wide family of channels.

In this paper, Section II reviews the singular value decomposition of the channel $\mathbf{H}$ matrices, while Section III uses a spatial keyhole example to demonstrate the degeneracy. Sections IV and V present and analyze the mechanisms by which channel degeneracy may arise in practical cases, Section IV for indoors (hallway) and Section V for outdoors. For simplicity, narrow-band capacity will be considered in this work. The results may readily be generalized to the wide-band case, simply by considering the wide-band as a collection of narrow-band channels.

II. Singular Value Decomposition

In general, for M transmitters and N receivers, the $N \times M$ channel matrix $\mathbf{H}$ may be represented in terms of the singular value decomposition (SVD): $\mathbf{H} = \mathbf{U}\mathbf{\Lambda}\mathbf{V}^{*}$ where $\mathbf{U}$ and $\mathbf{V}^{*}$ are unitary matrices with sizes $N \times N$ and $M \times M$, respectively, and $\mathbf{\Lambda}$ is an $N \times M$ diagonal matrix. Equivalently, the channel matrix $\mathbf{H}$ may be represented in terms of a sum of dyads

$$\mathbf{H} = \sum_{i}^{\min(N,M)} \mathbf{u}_i \lambda_i \mathbf{v}_i^{*} \tag{1}$$

where $\mathbf{u}_i$ and $\mathbf{v}_i$ are the ith row and column of $\mathbf{U}$ and $\mathbf{V}^{*}$, respectively, and * indicates a conjugate transpose. The singular value λ_i is proportional to the square root of the propagation loss. Each such dyad represents a mode of communication, or a degree of freedom. The form is suggestive of the sort of processing one might want to do at the transmitter (waterpouring) and at the receiver [10], [11].

III. Keyhole

Picture, for example, two-element transmitting and receiving arrays both surrounded by clutter. Ordinarily, this would lead to an uncorrelated Gaussian channel, which has been shown to have high capacity [1]. Now, imagine placing a screen with a small keyhole punched through it, separating the regions containing the receiving and transmitting arrays, as shown in Fig. 1. The only way for the radio wave to propagate to the receiver is to pass through the keyhole. The electric field incident on the keyhole is

$$E_{\text{inc}} = \begin{pmatrix} a_1 & a_2 \end{pmatrix} \begin{pmatrix} s_1 \\ s_2 \end{pmatrix} \tag{2}$$

where the channel coefficients a_1 and a_2 operate on the source signals s_1 and s_2. The channel coefficients include the effect of

Manuscript received August 15, 2000; revised December 27, 2000; accepted March 13, 2001. The editor coordinating the review of this paper and approving it for publication is P. F. Driessen.

The authors are with the Bell Laboratories, Crawford Hill Lab, Holmdel, NJ 07733 USA.

Publisher Item Identifier S 1536-1276(02)02926-4.

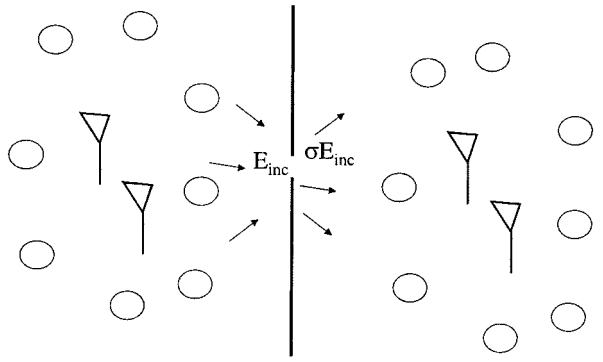

Fig. 1. Spatial keyhole concept.

rich multiple scattering and, therefore, are assumed to be distributed as independent Gaussian random variables. The field transmitted through the keyhole is σE_{inc}, where σ is the scattering cross section of the keyhole. The received field vector is

$$E_{\text{rec}} = \begin{pmatrix} b_1 \\ b_2 \end{pmatrix} \sigma E_{\text{inc}} \tag{3}$$

where b_1 and b_2 are complex Gaussian coefficients describing the scattering at the receive array. The channel matrix $\mathbf{H}$ is, thus, given by

$$\mathbf{H} = \begin{pmatrix} b_1 \\ b_2 \end{pmatrix} \sigma (a_1 \quad a_2) = \mathbf{b}\sigma\mathbf{a}^T = \sigma \begin{pmatrix} a_1 b_1 & a_2 b_1 \\ a_1 b_2 & a_2 b_2 \end{pmatrix} \tag{4}$$

which is clearly a dyad with one degree of freedom. As the coefficients a_1, a_2, b_1, and b_2 are independent, all entries of the channel matrix $\mathbf{H}$ are uncorrelated. Thus, the channel matrix has low correlation and yet a single degree of freedom. In contrast to the usual case, each entry of $\mathbf{H}$ is distributed not as a complex Gaussian but as a product of complex Gaussians. The probability distribution $f(p)$ of power p for such a process may be shown to be [12]

$$f(p) = \frac{2}{b^2} K_0 \left(\frac{2\sqrt{p}}{b} \right) \tag{5}$$

where b is the average power and K_0 is the modified Bessel function. This distribution is compared with the exponential distribution of power that characterizes complex Gaussian channels in Fig. 2. While, the vector nature of the electric field has been ignored here, the keyhole may be realized more generally by following the spatial keyhole by a polarizer, which suppresses one polarization. Multiple scattering may be written as a sum of "keyhole" cobtributions, Fig. 3, approaching a complex Gaussian process according to the Central Limit Theorem.

IV. Modal Keyhole in a Waveguide

The above presented the concept of a "spatial keyhole". Similar phenomena may be found in other basis. For example, Driessen and Foschini [5] have pointed out such degeneracy for large separation between transmit and receive arrays. Shiu *et al.* [6] has found similar behavior in the case of two rings of scatterers, at large separation. In that case, the single degree of freedom is supported by a "spectral keyhole" (i.e., single plane wave between the scattering regions). An example of a keyhole in a realistic environment arises in a hallway or a tunnel. At microwave frequencies the hallway may be thought

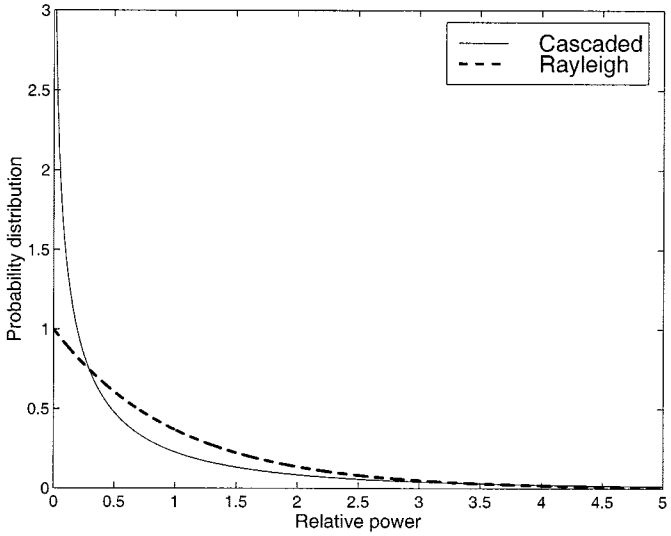

Fig. 2. Probability distributions of received signal power for a complex Gaussian and product of complex Gaussian processes.

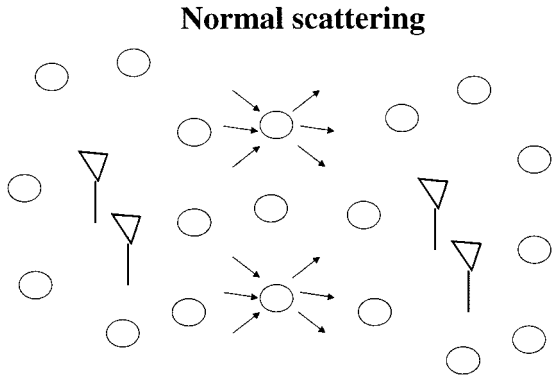

Fig. 3. Multiple "keyholes" or scatterers lead to a complex Gaussian process.

of as an overmoded waveguide. If the waveguide walls may be characterized by a perfectly conducting boundary condition and the cross section of the waveguide is homogeneously filled, the fields may be decomposed as a sum of transverse electric (TE) and transverse magnetic (TM) modes. The problem is then decomposed into two scalar problems. This case is treated in this section for simplicity. For antennas that are small relative to the wavelength, the entries h_{nm} of the $\mathbf{H}$ matrix may be modeled as responses to point sources. The coefficient h_{nm} which describes the propagation effects from transmitter m to receiver n obeys the Helmholtz scalar wave equation

$$\nabla^2 h_{nm} + k^2 h_{nm} = \delta \left(\underline{r}_n - \underline{\widehat{r}}_m \right) \tag{6}$$

and satisfies the boundary conditions on the walls of the waveguide. It may now be represented completely as a sum of normal modes with modal eigenfunctions $\phi_k(\underline{r}_n)$ corresponding to characteristic modal wavenumbers β_k where k is the mode index, and $r_n = (y_n, z_n)$ and $\widehat{r}_m = \left(\widehat{y}_m, \widehat{z}_m \right)$ are the coordinates of the receive antenna and transmit antennas, respectively, in the cross section of the waveguide

$$h_{nm} = \sum_k \phi_k(\underline{r}_n) \phi_k \left(\underline{\widehat{r}}_m \right) \frac{e^{i\beta_k x}}{2i\beta_k}. \tag{7}$$

The two arrays are separated by the distance x along the waveguide. A modal eigenfunction is a field solution to (6) that does not change its distribution in the cross section of the waveguide as the wave propagates. The received signal at a particular receiver consists of a sum of signals radiated by all the transmitters

$$r_n = \sum_m h_{nm} s_m = \sum_m \sum_k \phi_k(\underline{r}_i)\phi_k\left(\widehat{\underline{r}}_m\right) \frac{e^{i\beta_k x}}{2i\beta_k} s_m \quad (8)$$

where s_m is a signal applied to the mth transmit antenna. The vector of all the received signals is now

$$\begin{aligned}\underline{\mathbf{r}} &= \begin{pmatrix} r_1 \\ r_2 \\ \cdot \end{pmatrix} \\ &= \begin{pmatrix} \phi_1(\underline{r}_1) & \phi_2(\underline{r}_1) & \cdot \\ \phi_1(\underline{r}_2) & \phi_2(\underline{r}_2) & \cdot \\ \cdot & \cdot & \cdot \end{pmatrix} \begin{pmatrix} \frac{e^{i\beta_1 x}}{2i\beta_1} & 0 & \cdot \\ 0 & \frac{e^{i\beta_2 x}}{2i\beta_2} & \cdot \\ \cdot & \cdot & \cdot \end{pmatrix} \\ &\quad \times \begin{pmatrix} \phi_1\left(\widehat{\underline{r}}_1\right) & \phi_1\left(\widehat{\underline{r}}_2\right) & \cdot \\ \phi_2\left(\widehat{\underline{r}}_1\right) & \phi_2\left(\widehat{\underline{r}}_2\right) & \cdot \\ \cdot & \cdot & \cdot \end{pmatrix} \begin{pmatrix} s_1 \\ s_2 \\ \cdot \end{pmatrix} \end{aligned} \quad (9)$$

from where the channel transfer matrix may be written as a sum of dyads

$$\begin{aligned}\mathbf{H} &= \begin{pmatrix} \phi_1(\underline{r}_1) \\ \phi_1(\underline{r}_2) \\ \cdot \end{pmatrix} \frac{e^{i\beta_1 x}}{2i\beta_1} \begin{pmatrix} \phi_1\left(\widehat{\underline{r}}_1\right) & \phi_1\left(\widehat{\underline{r}}_2\right) & \cdot \end{pmatrix} \\ &+ \begin{pmatrix} \phi_2(\underline{r}_1) \\ \phi_2(\underline{r}_2) \\ \cdot \end{pmatrix} \frac{e^{i\beta_2 x}}{2i\beta_2} \begin{pmatrix} \phi_2\left(\widehat{\underline{r}}_1\right) & \phi_2\left(\widehat{\underline{r}}_2\right) & \cdot \end{pmatrix} + \cdots . \end{aligned} \quad (10)$$

The left and right vector components of any one of the dyads above are not necessarily orthogonal to the left and right vector components of other dyads. This is unlike the proper SVD decomposition in (1). Still, the number of modes supported by a waveguide limits maximum number of degrees of freedom. Correlation between antennas will reduce the capacity further. In the presence of loss, the lowest order mode dominates at large distances from the source. The channel for each polarization, thus, has only a single degree of freedom, represented by the lowest order mode—a "modal keyhole." Scattering in the waveguide regions surrounding both receiver and transmitter would not improve the richness of the channel. An example would be that of a signal propagating down a hallway and entering into a room with furniture. While the signals at different receivers may be uncorrelated, the capacity is reduced due to a fact that the signal has already gone through a modal keyhole.

More general waveguides are characterized by modes that are not TM or TE modes. While the mode functions may not be scalar in the coordinate system of the waveguide geometry, similar behavior is expected to arise there as well.

V. Outdoor Propagation

A. Origins of Angular Spread Outdoors

In the analysis carried out in this work, it is assumed that the dominant signal path suffers diffraction at the roof edge near the remote. It is also assumed that the angular spread, as perceived at the base station, originates due to scattering in the vicinity of the remote. No further scattering, e.g., from tall buildings around the base station, is assumed. It is important to determine whether there are significant paths that involve scattering from other buildings. In Jakes [13], the angular spread of the signal at the base station is related to the radius of the scatterers near the remote. Adachi *et al.* [16] have found that the apparent angular spread as perceived at the base station is related to the orientation of the street taken by the mobile. When the street with the mobile was running along a tangent to a circle centered at the base (circumferential route), the angular spread at the base was found to range from 2° to 6°. When the street was running along a radial line from the base (radial route), the angular spread was 1°–3°. The difference was explained by arguing that when taking the circumferential route, the mobile was surrounded by scatterers which were up and down the street, thus, producing a scattering radius that was much larger than that available at the radial route. Bertoni *et al.* [17] have also looked at the various mechanisms for producing the angular spread, but modeled primarily the scattering from buildings not necessarily close to the mobile. Furthermore, many successful physical (i.e., nonempirical) models of the propagation loss (e.g., Walfisch–Bertoni [18]) assume that the dominant signal travelling from the remote to the base is confined to the vertical plane, and suffers diffraction at the roof edge near the remote. For a vertical array, geometric arguments (Fresnel approximation) may be used to show that scattering in the horizontal plane, say from distant buildings, would produce a small contribution to capacity if the diffraction at the roof edge occurs near the remote.

B. Analysis

The diffracting edge acts as an equivalent horizontal line source with varying current strength along its length. If the base antennas are vertically separated, the richness of the perceived channel is collapsed, and a "keyhole" is formed. Increasing the vertical separation would not be of any use. This may be remedied by placing the base antennas in a horizontal array. In that case, adequate antenna separation will be required to assure low correlation [7]. Analysis demonstrating these effects follows below.

The environment is modeled as a dielectric slab, shown in Fig. 4, which represents large-scale clutter, e.g., houses, trees, etc. The signal radiated by the remote antennas is scattered in the vicinity of the remote and produces a field U in the horizontal plane lying above the street where the remote is located and at the height of the top of the large-scale clutter.

The scalar field U represents the horizontal H field in the case of vertical polarization and the horizontal E field in the case of horizontal polarization. This scalar field representation is strictly valid only where there is no cross-polarization coupling, but is used here for simplicity to demonstrate the effect of roof edge diffraction. It has been reported by Lee and Yeh [19] that cross-polarization coupling is about -6 dB in mobile radio. As the fading between the signals on the two polarizations is uncorrelated (Jakes [13]), the capacity is expected to be approximately doubled through the use of both polarizations at both the transmitter and the receiver. It is assumed that the medium has

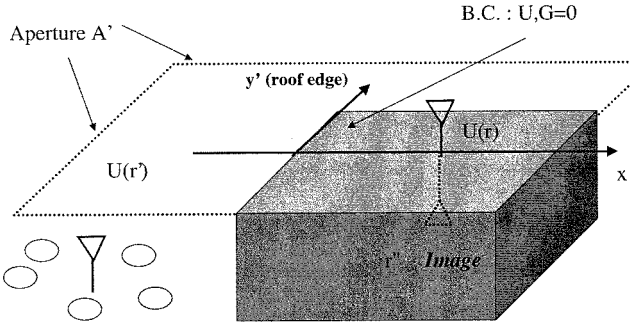

Fig. 4. Canonical outdoor environment.

no preferential treatment of either polarization [12]. The field U, therefore, satisfies the scalar Helmholtz equation

$$\nabla^2 U + k^2 U = 0. \tag{11}$$

The field radiated by the remote and measured at the base station may be expressed in terms of the values of the field at the boundary which is a horizontal plane just above the dielectric slab, by using Helmholtz–Kirchhoff theorem

$$U(\underline{r}) = \iint \underline{dA'} \cdot (U\nabla G - G\nabla U) \tag{12}$$

where the Green's function G is

$$G(r') = \frac{e^{ik|\underline{r}-\underline{r}'|}}{4\pi\,|\underline{r}-\underline{r}'|} - \frac{e^{ik|\underline{r}''-\underline{r}'|}}{4\pi\,|\underline{r}''-\underline{r}'|} \tag{13}$$

where $\mathbf{r}'$ points to the integration boundary, and $\mathbf{r}$ and $\mathbf{r}''$ point to the base station antenna and its image, respectively. The Green's function is the field response at $\mathbf{r}'$ due to a point source at $\mathbf{r}$. It serves a role similar to the impulse response in linear system theory, while (12) may be thought of as a superposition integral. In (12), the integration is over the horizontal plane boundary. Both the field U and the Green's function G satisfy the Dirichlet boundary condition at the top of the large-scale clutter: $U = 0$, $G = 0$. This is approximately true for both horizontal and vertical polarizations for plane wave reflection from a dielectric half space when the grazing angles are small. This is the case of interest in terrestrial communications, where the height of the base station is small compared with the distance to the remote.

As the Green's function G is zero over the entire boundary, the second term in the integrand of (12) drops out and the integration in (12) is then over the horizontal half-plane to the left of the gray region in Fig. 4. The field at the base may then be calculated as

$$U(\underline{r}) = \frac{ize^{ikx}}{\lambda x^2} e^{ik(z^2+y^2)/2x} \int_{-\infty}^{\infty} dy' \int_{-\infty}^{0} dx' U(x', y', 0) \times \exp\left(-ikx' + \frac{iky'^2}{2x} - \frac{ikyy'}{x}\right) \tag{14}$$

where λ is the wavelength. The Fresnel approximation for the distance R between the base antenna (or its image) and the aperture has been employed in (14)

$$\begin{aligned} R &= \sqrt{(x-x')^2 + (y-y')^2 + (z-z')^2} \\ &\approx (x-x') + \frac{(y-y')^2 + (z-z')^2}{2x}. \end{aligned} \tag{15}$$

For the high frequencies considered here the wavenumber k is high and most of the contribution to the integral over x' in (14) comes from the neighborhood of $x' = 0$. Equation (14) may be simplified by evaluating the integral over the x' coordinate by means of the initial value theorem

$$U(\underline{r}) = \frac{ze^{ikx}}{\lambda x^2 k} e^{ik(z^2+y^2)/2x} \int_{-\infty}^{\infty} dy' U(0, y', 0) \times \exp\left(\frac{iky'^2}{2x} - \frac{ikyy'}{x}\right). \tag{16}$$

Now the integral is only over the y' axis which coincides with the roof edge. Equation (16) expresses the fact that the field U measured at the base results from the diffraction of the remote field at the roof edge. Note that the received power P_R may be expressed in terms of the field U as

$$P_R = P_T \lambda^2 |U(\underline{r})|^2 G_T G_R \tag{17}$$

where G_T is the transmitter gain, G_R is the receiver gain, and P_T is the transmitted power. Using (16) for the field U, one finds that the received power P_R varies with frequency and distance to the base station in a way that is comparable to the empirical Hata model [20]. In particular, the received signal power decays with distance x as $1/x^4$.

For an array of base antennas that are all located at the same distance x from the roof edge, the vector of received signals is

$$\mathbf{r} \sim \mathbf{U} = \frac{e^{ikx}}{\lambda x^2 k} \times \begin{pmatrix} z_1 e^{ikz_1^2/2x} \int_{-\infty}^{\infty} dy' U(0, y', 0) e^{ik(y_1 - y')^2/2x} \\ z_2 e^{ikz_2^2/2x} \int_{-\infty}^{\infty} dy' U(0, y', 0) e^{ik(y_2 - y')^2/2x} \\ \vdots \end{pmatrix} \tag{18}$$

where the edge field $U(0, y', 0)$ is

$$\begin{aligned} U(0, y', 0) &= G_1(0, y', 0) s_1 + G_2(0, y', 0) s_2 + \cdots \\ &= \begin{pmatrix} G_1(0, y', 0) & G_2(0, y', 0) & \cdot \end{pmatrix} \begin{pmatrix} s_1 \\ s_2 \\ \cdot \end{pmatrix} \end{aligned} \tag{19}$$

and $G_m(0, y', 0)$ is the Green's function due to the source m which is evaluated at the roof edge, and includes all the street-level scattering, and s_m is the signal transmitted from the source m. We can now write the channel transfer function $\mathbf{H}$ as shown in (20) at the bottom of the page.

$$\mathbf{H} = \frac{e^{ikx}}{\lambda x^2 k} \begin{pmatrix} z_1 e^{ikz_1^2/2x} \int_{-\infty}^{\infty} dy' G_1(0, y', 0) e^{ik(y_1 - y')^2/2x} & z_1 e^{ikz_1^2/2x} \int_{-\infty}^{\infty} dy' G_2(0, y', 0) e^{ik(y_1 - y')^2/2x} & \cdot \\ z_2 e^{ikz_2^2/2x} \int_{-\infty}^{\infty} dy' G_1(0, y', 0) e^{ik(y_2 - y')^2/2x} & z_2 e^{ikz_2^2/2x} \int_{-\infty}^{\infty} dy' G_2(0, y', 0) e^{ik(y_2 - y')^2/2x} & \cdot \\ \vdots & \vdots & \vdots \end{pmatrix}. \tag{20}$$

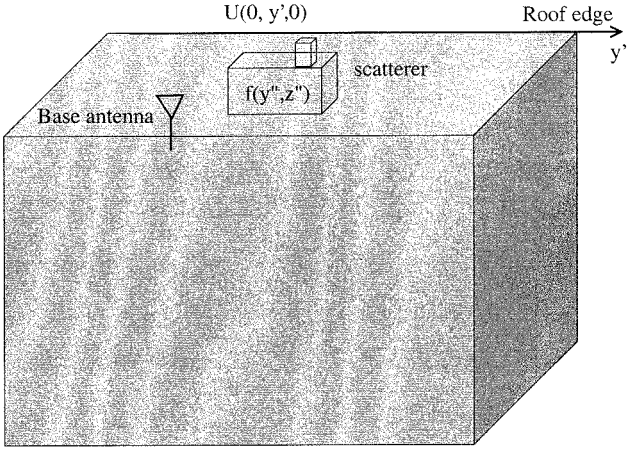

Fig. 5. Effect of additional scattering such as from a tall building over the rooftops.

C. Vertical Base Array

When the base antennas are arranged in a vertical array, $(x_n, y_n, z_n) = (x, y, z_n)$ for all n, where n is the base antenna index. Using these coordinates in (20) the channel transfer matrix may then be immediately written as shown in (21) at the bottom of the page. Note that the $\mathbf{H}$ matrix is a dyad, providing only a single degree of freedom. This degenerate behavior results from applying the initial value theorem to (14) to get (16). The resulting field as measured at the base station has lost all richness in the vertical direction.

We now try to generalize to include additional scattering over the slab representing the large-scale clutter. The scattering is represented by the scattering amplitude $f(x, y)$, shown in Fig. 5. The field received by a base antenna l due to remote antenna m is

$$U_m(x, y, z_l) = \frac{z_1 e^{ik(x-x'')}}{\lambda(x-x'')^2 k} \int_S dz'' \int_S dy'' U_{\mathbf{inc}_m}(x'', y'', z'') \times e^{ik(y-y'')^2/2(x-x'')} e^{ik(z_1-z'')^2/(2(x-x'')} f(y'', z''). \quad (22)$$

The field incident on the scatterer is $U_{\mathbf{inc}_m}(x'', y'', z'')$ which is the field radiated by the remote source m, scattered at street level and diffracted over the roof edge. The integration is carried out over the scatterer whose coordinates are double primed. We can use (16) to determine $U_{\mathbf{inc}}$ in (22). For separable scattering amplitude $f(y'', z'') = f(y'')f(z'')$, we get the channel transfer matrix $\mathbf{H}$ as shown in (23) at the bottom of the page.

The received signal is still a dyad with one degree of freedom. If the scattering strength $f(y'', z'')$ is not separable, the propagation is no longer strictly degenerate. The capacity would then depend on the ability of the base station array to resolve adequately the scattered signals, which may be difficult in the vertical plane where the angle spreads tend to be small [16]. The impact on capacity may be quantified for a particular scattering geometry through a correlation matrix [7].

D. Horizontal Base Array

When the base antennas are arranged in a horizontal linear array, the x and z coordinates are the same for all the elements $(x_n, y_n, z_n) = (x, y_n, z)$. From (18), the receive signal vector may be written as

$$\mathbf{r} \sim \mathbf{U} = \frac{e^{ikx}}{\lambda x^2 k} z e^{ikz^2/2x} \begin{pmatrix} \int_{-\infty}^{\infty} dy' U(0, y', 0) e^{ik(y_1-y')^2/2x} \\ \int_{-\infty}^{\infty} dy' U(0, y', 0) e^{ik(y_2-y')^2/2x} \\ \vdots \end{pmatrix} \quad (24)$$

and the $\mathbf{H}$ matrix is shown in (25) at the bottom of the next page. It may be observed that it is not possible to factor the $\mathbf{H}$ matrix in the same way as was done in the case of the vertical array in (21). The integration carried out in (24) and (25) may be seen to be a linear (and unitary) transformation of the roof edge field $U(0, y', 0)$ and the Green's function G, respectively. As the field at the roof edge has undergone extensive scattering in the vicinity of the remote, the field at the roof edge is actually a sum of many multipath arrivals, and may be modeled as a complex Gaussian process, following the central limit theorem. Received field $U(\underline{\mathbf{r}})$ is a linear functional of aperture field $U(\underline{\mathbf{r}}')$, as seen in (14). If $U(\underline{\mathbf{r}}')$ is a Gaussian process, so is $U(\underline{\mathbf{r}})$, because a linear transformation of a Gaussian process is also Gaussian. Gaussian processes are completely characterized by their mean and covariance.

The antenna elements at the remote are assumed to be adequately separated to produce no correlation between the remote antennas (antenna separation on the order of $\lambda/2$ for isotropic scattering). Thus, the Green's functions $G_m(0, y', 0)$ and $G_p(0, y', 0)$ are not correlated for any $m \neq p$ and, alternatively, entries of $\mathbf{H}$ which are in different columns are uncorrelated.

$$\mathbf{H} = \begin{pmatrix} z_1 e^{ikz_1^2/2x} \\ z_2 e^{ikz_2^2/2x} \\ \vdots \end{pmatrix} \frac{e^{ikx}}{\lambda x^2 k} \left(\int_{-\infty}^{\infty} dy' G_1(0, y', 0) e^{ik(y-y')^2/2x} \quad \int_{-\infty}^{\infty} dy' G_2(0, y', 0) e^{ik(y-y')^2/2x} \quad \cdot \right). \quad (21)$$

$$\mathbf{H} = \begin{pmatrix} z_1 \int_S dz'' z'' e^{ikz''^2/2x''} e^{ik(z_1-z'')^2/2(x-x'')} f(z'') \\ z_2 \int_S dz'' z'' e^{ikz''^2/2x''} e^{ik(z*_2-z'')^2/2(x-x'')} f(z'') \\ \vdots \end{pmatrix} \frac{e^{ikx}}{(\lambda k)^2 x''^2 (x-x'')^2} \times \left(\int_S dy'' \int_{-\infty}^{\infty} dy' U_1(0, y', 0) e^{ik(y''-y')^2/2x''} e^{ik(y-y'')^2/2(x-x'')} f(y'') \right. \left. \int_S dy'' \int_{-\infty}^{\infty} dy' U_2(0, y', 0) e^{ik(y''-y')^2/2x''} e^{ik(y-y'')^2/2(x-x'')} f(y'') \quad \cdot \right) \quad (23)$$

The only correlations that need be computed are between the entries in different rows but the same column of $\mathbf{H}$.

Now the mean of the field at the base due to remote antenna m is computed by taking the average of any element of (25)

$$\begin{aligned}\langle U_m(\underline{r})\rangle =& \frac{ze^{ikx}}{\lambda x^2 k} e^{ik(z^2+y^2)/2x} \int_{-\infty}^{\infty} dy' \langle G_m(0,y',0)\rangle \\ & \times \exp\left(\frac{iky'^2}{2x} - \frac{ikyy'}{x}\right) \\ =& 0. \end{aligned} \tag{26}$$

The mean field at the receiver is found to be zero, provided the mean field at the roof edge is zero, $\langle G_m(0,y',0)\rangle = 0$.

Next the correlation of the field due to source m measured at the two base antennas $\langle U_m(\underline{r}_1)U_m(\underline{r}_2)^*\rangle$ may be determined from two entries of (25) that are in the same column m as shown in (27) at the bottom of the page. For convenience, the coordinate system in both the primed (aperture) and unprimed (base) locations has been changed to the center and difference coordinates, denoted by the subscripts c and d. Correlation at the base station is seen to be a linear functional of correlation at the aperture. Through the integral in (27), the correlation function of the field at the roof edge may be propagated to the base station antennas.

We can proceed further by making a particular assumption about the form of the correlation function of the field at roof edge. The correlation of the field at two points on the roof edge is represented by a delta function in the difference coordinate, which simply means that the fields at two distinct points are assumed to be uncorrelated. This is an approximation which is thought to be valid as the field is expected to be decorrelated on a scale of $\lambda/2$ which is much smaller than other spatial scales in (27).

The field of remote antenna m at the roof edge is then represented by an incoherent line source of intensity $I(y'_c)$ at the roof edge

$$\left\langle G_m(0,y',0)G_m(0,y'',0)^*\right\rangle = \frac{4\pi^2}{k^2} I(y'_c)\,\delta(y'_d). \tag{28}$$

Substituting (28) into (27), we get

$$\begin{aligned}\left\langle U_m(\underline{r}_1)U_m(\underline{r}_2)^*\right\rangle =& \frac{z_1 z_2 e^{i(k/2x)\left(z_1^2-z_2^2\right)} e^{\frac{ik}{x}y_c y_d}}{\lambda^2 k^2 x^4} \\ & \times \int_{-\infty}^{\infty} dy'_c \frac{4\pi^2}{k^2} I(y'_c)\, e^{(-ik/x)y'_c y_d}. \end{aligned} \tag{29}$$

If we assume the incoherent intensity to be of Gaussian form with the spatial scale σ_y of the order of street width

$$I(y'_c) = \sqrt{\frac{1}{2\pi\sigma_y^2}} \exp\left(-\frac{y'^2_c}{2\sigma_y^2}\right). \tag{30}$$

Correlation coefficient, obtained by normalizing (29), is also of Gaussian form

$$\rho(y_d) = \frac{\left\langle U_m(\underline{r}_1)U_m(\underline{r}_2)^*\right\rangle}{\sqrt{\left\langle \left|U_m(\underline{r}_1)\right|^2\right\rangle \left\langle \left|U_m(\underline{r}_2)\right|^2\right\rangle}} = \exp\left(-\frac{k^2\sigma_y^2 y_d^2}{2x^2}\right) \tag{31}$$

where y_d is the distance between base antennas. The correlation coefficient in (31) is compared in Fig. 6 to the correlation coefficient, which results from the analysis by Chu and Greenstein [14] of the empirical data, collected by Rhee and Zysman [15]. The spatial scale of 30 meters (m) corresponds well to the 2° spread observed for remote locations 1 km away.

Now the stochastic process determining the channel transfer matrix $\mathbf{H}$ is completely specified. Given the assumptions in this section, and for the case of the horizontal base array, the $\mathbf{H}$ process is seen to be a complex Gaussian process with matrix mean zero, which follows from (26), and zero covariance between distinct remote antennas $\langle h_{im}h^*_{kl}\rangle = 0$ for $m \neq l$, which is a consequence of the delta function dependence in (28). For a system with N remote antennas and M base station antennas, the random $\mathbf{H}$ matrix may then be generated from $\mathbf{H} = \sqrt{\mathbf{C}}\mathbf{H}_{\text{iid}}$, where $\mathbf{H}_{\text{iid}}$ is a matrix of independent identically distributed complex Gaussian entries, and $\mathbf{C}$ is the $M \times M$ covariance matrix with entries $c_{\text{nk}} = \langle h_{nm}h^*_{km}\rangle = \rho(y_{\text{nk}})$, where ρ is given by (31), and y_{nk} is the horizontal separation between base station antennas n and k. Here, both $\mathbf{H}$ and $\mathbf{H}_{\text{iid}}$ are $M \times N$ matrices, and the matrix square root is the square root with nonnegative eigenvalues. In [7], the capacity of the

$$\mathbf{H} = \frac{e^{ikx}}{\lambda x^2 k} z e^{ikz^2/2x} \begin{pmatrix} \int_{-\infty}^{\infty} dy' G_1(0,y',0) e^{ik(y_1-y')^2/2x} & \int_{-\infty}^{\infty} dy' G_2(0,y',0) e^{ik(y_1-y')^2/2x} & \cdot \\ \int_{-\infty}^{\infty} dy' G_1(0,y',0) e^{ik(y_2-y')^2/2x} & \int_{-\infty}^{\infty} dy' G_2(0,y',0) e^{ik(y_2-y')^2/2x} & \cdot \\ \vdots & \vdots & \vdots \end{pmatrix}. \tag{25}$$

$$\begin{aligned}\left\langle U_m(\underline{r}_1)U_m(\underline{r}_2)^*\right\rangle =& \frac{z_1 z_2 e^{i(k/2x)\left(z_1^2-z_2^2\right)} e^{(ik/x)y_c y_d}}{\lambda^2 k^2 x^4} \\ & \times \int_{-\infty}^{\infty}\int_{-\infty}^{\infty} dy'_c dy'_d \left\langle G_m\left(0, y'_c + \frac{y'_d}{2}, z_1\right) G_m^*\left(0, y'_c - \frac{y'_d}{2}, z_2\right)\right\rangle e^{(-ik/x)\left(y'_c y_d + y_c y'_d\right)} e^{(ik/x)y'_c y'_d} \\ y'_c =& \frac{y'+y''}{2}, \quad y'_d = y' - y'', \\ y_c =& \frac{y_1+y_2}{2}, \quad y_d = y_1 - y_2. \end{aligned} \tag{27}$$

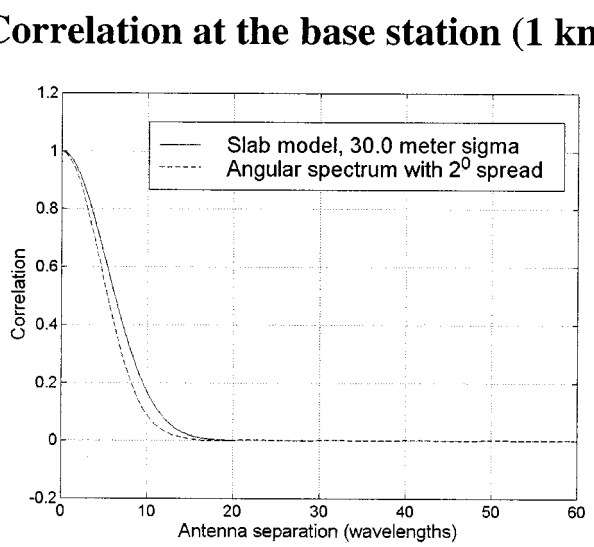

Fig. 6. Correlation of signals received at the base station antennas as a function of separation. Compared are correlation coefficient computed under the assumption of limited angular spectrum with a 2° spread ([4], [8]) and correlation coefficient from (31).

channel has been analyzed in the case when there is a correlation between the signals received at the base station antennas. The correlation coefficient between antennas has been derived based on the assumption that the angular spectrum of signals received at the base is of width 2° at 1 km. This is seen in Fig. 6 to be equivalent to the correlation coefficient obtained in the analysis in this work. The results in [7] may, therefore, be applied here without reservation. It was found that, when the base antennas are separated by 4λ, the capacity at 10% outage is 80% of that achievable in completely uncorrelated Gaussian channels. This appears to be a reasonable compromise between base antenna array size and achievable capacity.

E. Discussion

Above it was found that a vertical array at the base station would perceive a keyhole due to the diffraction at the roof edge near the mobile. A horizontal array, however, would not perceive a keyhole, and would, thus, achieve higher capacity, provided the antennas are adequately separated. The anomalous behavior of the vertical array arises only if all other paths, such as around the buildings, are negligible compared with the one that diffracted over the roof edge. Such additional scattering will, generally, increase the richness of the channel, thus, increasing the channel capacity. While the degeneracy of the channel in the case of a roof edge diffraction and a vertical base array does not hold strictly once the nonseparable scatter (e.g., from tall buildings) is included, the capacity is still expected to be low, as the vertical array would have to resolve in the vertical plane signals that have mostly been scattered in the horizontal plane. A conservative model would nevertheless attribute the angular spread to the scattering in the vicinity of the remote, ruling out the use of a vertical base station array, as was done here. For a horizontal array, additional scattering from tall buildings would enrich the channel and lead to larger capacities.

VI. Conclusion

It was shown here that degenerate channel phenomena, called "keyholes" may arise under realistic assumptions which have zero correlation between the entries of the channel matrix $\mathbf{H}$ and yet only a single degree of freedom. Decorrelation is, therefore, not a guarantee of BLAST performance. Such cases lead to the entries of the $\mathbf{H}$ matrix following statistics that are a product process of two complex Gaussian distributions, as opposed to the complex Gaussian distribution normally assumed in wireless channels. Canonical physical examples of keyholes have been demonstrated, including a spatial keyhole in a metal screen, a modal keyhole in a waveguide, or a hallway (when only one mode propagates). Of most relevance to outdoor propagation, a diffraction-induced keyhole that is perceived by a vertical base array has been discussed and modeled in detail. A remedy for this degeneracy is to use a horizontal array, where the antenna elements are separated enough to resolve the scattering region around the remote. In previous work, it was found to be sufficient to separate the elements by 4λ, provided the scattering region is about 30 m in diameter (about a street width), and the remote is less than 1 km away from the base. A similar diffraction-induced keyhole might occur in a microcell system in the case of a vertical building edge and a horizontal array, as may be found in a microcell. Such degeneracy would be removed if there are other paths (e.g., reflection paths) beside the diffracted ray. Finally, a nightmare scenario may be envisioned where the dominant signal from the remote is first diffracted at the roof edge and then around the vertical edge of a tall building on its way to the base station. In this case, a roof edge would collapse all the vertical richness of the channel, as above, and then a vertical building edge would subsequently collapse all the horizontal richness. This would leave only two degrees of freedom for two polarizations, which may be further collapsed to one degree of freedom after passage through a polarizing medium, such as a metal picket fence. Such a scenario is conceivable but may be argued to be somewhat contrived.

References

[1] G. J. Foschini and M. J. Gans, "On limits of wireless communications in a fading environment when using multiple antennas," *Wireless Personal Commun.*, vol. 6, Mar. 1998.

[2] G. J. Foschini, "Layered space-time architecture for wireless communication in a fading environment when using multiple antennas," *Bell Labs Tech. J.*, vol. 1, pp. 41–59, 1996.

[3] G. D. Golden, G. J. Foschini, R. A. Valenzuela, and P. W. Wolniansky, "Detection algorithm and initial laboratory results using the V-BLAST space–time communication architecture," *Electron. Lett.*, vol. 35, pp. 14–15, Jan. 1999.

[4] P. W. Wolniansky, G. J. Foschini, G. D. Golden, and R. A. Valenzuela, "V-BLAST: An architecture for realizing very high data rates over the rich-scattering wireless channel," presented at the ISSSE-98, Sept. 1998.

[5] P. F. Driessen and G. J. Foschini, "On the capacity formula for multiple input–multiple output wireless channels: A geometric interpretation," *IEEE Trans. Commun.*, vol. 47, pp. 173–176, Feb. 1999.

[6] D.-S. Shiu, G. J. Foschini, M. J. Gans, and J. M. Kahn, "Fading correlation and its effect on the capacity of multielement antenna systems," *IEEE Trans. Commun.*, vol. 48, pp. 502–513, Mar. 2000.

[7] D. Chizhik, F. Rashid-Farrokhi, J. Ling, and A. Lozano, "Effect of antenna separation on the capacity of BLAST in correlated channels," *IEEE Commun. Lett*, vol. 4, pp. 337–339, Nov. 2000.

[8] D. Chizhik, G. J. Foschini, and R. A. Valenzuela, "Capacities of multielement transmit and receive antennas: Correlations and keyholes," *IEE Electron. Lett.*, vol. 36, pp. 1099–1100, June 2000.

[9] D. Gesbert, H. Bolcskei, D. Gore, and A. Paulraj, "MIMO wireless channels: Capacity and performance prediction," in *Proc. CT10-5, IEEE Globecom 2000*, San Francisco, CA, Nov. 27–Dec. 1, 2000.
[10] F. R. Farrokhi, G. J. Foschini, A. Lozano, and R. A. Valenzuela, "Link-optimal space-time processing with multiple transmit and receive antennas," IEEE Commun. Lett., to be published.
[11] G. G. Raleigh and J. M. Cioffi, "Spatio-Temporal coding for wireless communications," *IEEE Trans. Commun.*, vol. 46, pp. 357–366, Mar. 1998.
[12] V. Erceg, S. J. Fortune, J. Ling, A. J. Rustako Jr, and R. A. Valenzuela, "Comparison of WiSE propagation tool prediction with experimental data collected in urban microcellular environments," *IEEE J. Select. Areas Commun.*, vol. 15, pp. 677–684, May 1997.
[13] W. C. Jakes, Ed., *Microwave Mobile Communications*. New York: Wiley, 1974.
[14] T.-S. Chu and L. J. Greenstein, "A semiempirical representation of antenna diversity gain at cellular and PCs base stations," *IEEE Trans. Commun.*, vol. 45, June 1997.
[15] S. B. Rhee and G. I. Zysman, "Result of suburban base station diversity measurements in the UHF band," *IEEE Trans. Commun.*, vol. COM–22, pp. 1630–1636, Oct. 1974.
[16] F. Adachi, M. T. Feeney, A. G. Williamson, and J. D. Parsons, "Cross-correlation between the envelopes of 900 MHz signals received at a mobile radio base station site," *Proc. Inst. Elect. Eng.*, pt. F, vol. 133, pp. 506–512, Oct. 1986.
[17] H. L. Bertoni, P. Pongsilamanee, C. Cheon, and G. Liang, "Sources and statistics of multipath arrival at elevated base station antenna," in *Proc. IEEE 49th Vehicular Technology Conf.*, Houston, TX, May 16–20, pp. 581–585.
[18] J. Walfisch and H. L. Bertoni, "A theoretical model of UHF propagation in urban environments," *IEEE Trans. Antennas Propagat.*, vol. AP-36, pp. 1788–1796, Dec. 1988.
[19] W. C.-Y. Lee and Y. S. Yeh, "Polarization diversity system for mobile radio," *IEEE Trans. Commun.*, vol. COM-20, pp. 912–923, Oct. 1972.
[20] M. Hata, "Empirical formula for propagation loss in land mobile radio services," *IEEE Trans. Veh. Technol.*, vol. VT–29, Aug. 1980.

Dmitry Chizhik received the Ph.D. degree in electrophysics at the Polytechnic University, Brooklyn, NY. His thesis work was on ultrasonics and nondestructive evaluation.

In 1991, he joined the Naval Undersea Warfare Center, New London, CT, where he did research in scattering from ocean floor and shallow water acoustic propagation. In 1996, he joined Bell Laboratories, Lucent Technologies, Holmdel, NJ, working on radio-propagation modeling and measurements using deterministic and statistical techniques. His recent work has been in measurement and modeling of MIMO channels. The results are used for both determination of channel-imposed bounds on channel capacity and for optimal antenna array design.

Gerald J. Foschini (S'60–M'62–SM'83–F'86) received the B.S.E.E. degree from New Jersey Institute of Technology (NJIT), Newark, NJ, the M.E.E. degree from New York University, New York, and the Ph.D. degree in mathematics from Stevens Institute, Hoboken, NJ.

He has been involved with data communications research on many kinds of systems including wireless communications and optical communications systems. He has done research on point-to-point systems as well as on networks. He has taught at Princeton University, Princeton, NJ and Rutgers University, Piscataway, NJ.

Michael J. Gans (S'60–M'66–SM'84–F'93) received the Ph.D. degree in electrical engineering from the University of California at Berkeley, in 1965.

He is on the staff of the Wireless Communications Research Department at Bell Labs, Holmdel, NJ. He has been at Bell Laboratories since 1966. His primary technical areas include mobile radio, antennas, satellites, fiber optics, and infrared communications.

Reinaldo A. Valenzuela (M'85–SM'89–F'99) received the B.S. degree from University of Chile, Santiago, and the Ph.D. degree from Imperial College of Science and Technology of the University of London, U.K.

At Bell Laboratories, he studied indoor microwave propagation and modeling, packet reservation multiple access for wireless systems and optical wavelength division multiplexing (WDM) networks. He became Manager of the Voice Research Department at Motorola Codex, Boston, MA, where he was involved in the implementation of integrated voice and data packet systems. On returning to Bell Laboratories, he led a multidisciplinary team to create a software tool for wireless system engineering (WiSE), now in widespread use in Lucent Technologies. He received the Distinguished Member of Technical Staff award and is Director of the Wireless Communications Research Department. He is interested in microwave propagation measurements and models, intelligent antennas, third-generation wireless system, and space–time systems achieving high capacities using transmit and receive antenna arrays. He has published over 80 papers and holds 12 patents.

Dr. Valenzuela is editor for the IEEE TRANSACTIONS ON COMMUNICATIONS and the IEEE TRANSACTIONS ON WIRELESS COMMUNICATIONS.